JACS
JOURNAL OF THE AMERICAN CHEMICAL SOCIETY
Cite This: J. Am. Chem. Soc. 2019, 141, 13003−13007
Communication
pubs.acs.org/JACS

Designing Open Metal Sites in Metal−Organic Frameworks for Paraffin/Olefin Separations

Mona H. Mohamed,[†,‡] Yahui Yang,[§] Lin Li,[§] Sen Zhang,[§] Jonathan P. Ruffley,[§] Austin Gamble Jarvi,[†] Sunil Saxena,[†] Götz Veser,[*,§] J. Karl Johnson,[*,§] and Nathaniel L. Rosi[*,†,§]

[†]Department of Chemistry, University of Pittsburgh, Pittsburgh, Pennsylvania 15261, United States
[‡]Chemistry Department, Faculty of Science, Alexandria University, P.O. Box 426, Ibrahimia, Alexandria 21321, Egypt
[§]Department of Chemical & Petroleum Engineering, University of Pittsburgh, Pittsburgh, Pennsylvania 15261, United States

Supporting Information

ABSTRACT: Incorporating open metal sites (OMS) into metal−organic frameworks allows design of well-defined binding sites for selective molecular adsorption, which has a profound impact on catalysis and separations. We demonstrate that Cu(I) sites incorporated into MFU-4*l* preferentially adsorb olefins over paraffins. Density functional theory (DFT) calculations show that the OMS are independent, with no dependence of binding energy on olefin loading up to one olefin per Cu(I). Experimentally, increasing Cu(I) loading increased olefin uptake without affecting the binding energy, as predicted by DFT and confirmed by temperature-programmed desorption. The potential of this material for olefin/paraffin separation under ambient conditions was investigated by gas adsorption and column breakthrough experiments for an equimolar ratio of olefin/paraffin. High-grade propylene and ethylene (>99.999%) can be generated using temperature−concentration swing recycling from a Cu(I)-MFU-4*l* packed column with no measurable paraffin breakthrough.

Isolated open metal sites (OMS) are an active area of investigation due to their significance in single-site catalysis, chromic sensors, and gas adsorption and separation.[1−5] Electron-rich transition metals are known to bind strongly to unsaturated carbon−carbon bonds through both σ- and π-backbonding interactions.[6] Hence, selective adsorption of olefins onto materials bearing OMS could enable separation of olefins and paraffins, which is industrially achieved through energy-intensive high-pressure cryogenic distillation estimated to consume ∼800 PJ of energy for the global annual production of ethylene of 152 MMT.[7−10]

Metal−organic frameworks (MOFs) are highly modular sorbents showing promise for many adsorption-based molecular separations.[9,11−19] Their high crystallinity makes them ideal materials for incorporation of OMS.[20,21] The unique advantage of using MOFs with OMS for separation processes is the single-site nature of the material, which offers a greater level of control over the selectivity compared to a sorbent with heterogeneous binding sites. The high crystallinity and vast chemical design space of MOFs lends itself to computational modeling and screening to direct the design of task-specific materials. In this work, we report a combined theory and experimental approach to examine the application of Cu(I) OMS in MFU-4*l* (Metal−Organic Framework Ulm University-4large) for the separation of olefins from paraffins.

MFU-4*l* has been used to immobilize metal active sites for catalysis.[22−26] Its structure (Figure 1a) consists of $Zn_5Cl_4(ta)_6$ (ta = triazolate) units bridged by the dibenzo-1,4-dioxin portion of the bis(1,2,3-triazolato-[4,5-*b*],[4′,5′-i])dibenzo-[1,4]-dioxin (BTDD) ligands. These clusters contain one core octahedral Zn(II) and four periphery tetrahedral Zn(II) (Figure 1b). OMS can be generated in the peripheral positions by replacing Zn(II) via cation exchange.

Density functional theory (DFT) calculations on full periodic structures of MFU-4*l*, with and without Cu(I) substitution, were performed using the Bayesian error estimation functional van der Waals (BEEF vdW) approach[27] and then validated by comparing binding energies from DFT and experiments (Supporting Information). A large difference in relative adsorption energies is required for efficient separations relying on competitive binding. To estimate the ease of separation, we performed DFT calculations for the adsorption of C2−C4 olefins and paraffins in Cu(I)-MFU-4*l*, in which a single Zn(II)-Cl was replaced with a single tricoordinate Cu(I). The optimized geometry of an adsorbed ethylene on the Cu(I) site is shown in Figure 1c.

More importantly, we computed the differences in binding energies between olefin/paraffin pairs, including uncertainty quantification of these energy differences. The uncertainty analysis was generated using the BEEF-ensemble,[27] which estimates uncertainties in DFT calculations due to the choice of exchange-correlation functionals.[27] The binding energy differences are −0.60 ± 0.10, −0.49 ± 0.14, −0.51 ± 0.13, and −0.43 ± 0.16 eV for ethylene/ethane, propylene/propane, 1-butene/butane, and 2-*trans*-butene/butane, respectively (Figure 1d,e and Figure S2). Thus, DFT predicts with high confidence that a wide range of olefin/paraffin separations will be very efficient in Cu(I)-MFU-4*l*. In contrast, binding energies of olefin/paraffin pairs in unsubstituted MFU-4*l* are essentially identical (no separation). The adsorbates in unsubstituted MFU-4*l* physisorb close to the 3-fold center of the node, instead of the Zn(II)-Cl peripheral site (Figure S4).

Received: June 20, 2019
Published: August 5, 2019

DOI: 10.1021/jacs.9b06582
J. Am. Chem. Soc. 2019, 141, 13003−13007

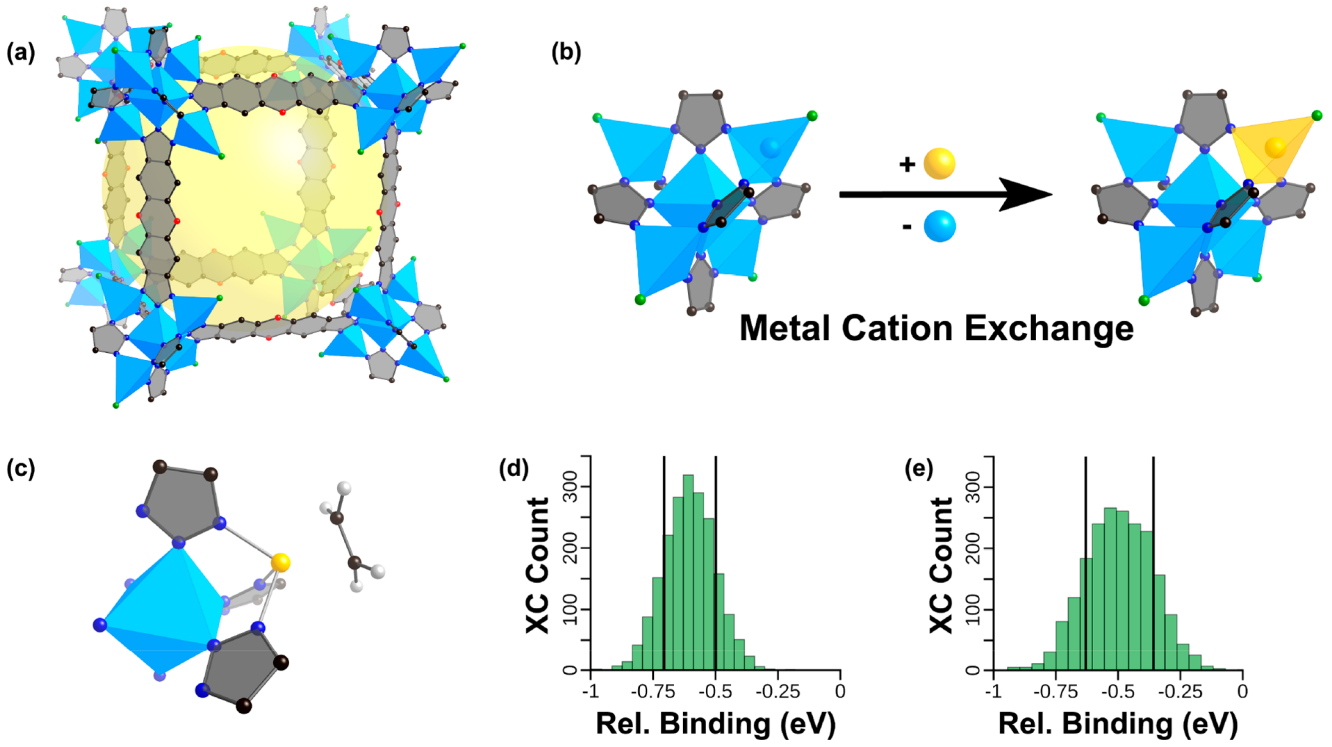

Figure 1. (a) Crystal structure of MFU-4*l* (Zn, light blue; Cl, green; N, dark blue; O, red; C, charcoal; H omitted for clarity). (b) Schematic showing the replacement of a peripheral tetrahedral Zn(II) cation with another metal cation via cation exchange (Cu, yellow). (c) Optimized binding geometry of ethylene to the Cu(I) site. (d) Histogram plots of the energy differences for ethylene/ethane and (e) propylene/propane binding energies as computed from the BEEF vdW ensemble. XC Count is the exchange-correlation count. Vertical lines represent ± one standard deviation in the BEEF ensemble. Negative values indicate a preference for alkene binding over alkane.

Importantly, our DFT calculations show that the binding of ethylene on Cu(I)-MFU-4*l* with all peripheral sites substituted with Cu(I) is essentially the same as for a single substituted site (*vide infra*). Taken together, these calculations (i) show a dramatic difference in binding of a wide range of olefins and paraffins to the Cu(I) site; (ii) predict that the optimal material is achieved by replacing all Zn(II)-Cl with Cu(I); and (iii) underscore the promise of Cu(I)-MFU-4*l* for olefin–paraffin separations.

Motivated by these findings, we targeted Cu(I)-MFU-4*l* variants with different loadings of Cu(I) OMS to evaluate the effect of OMS concentration on olefin/paraffin separation performance. We adapted an established synthetic procedure[28] (Supporting Information), varying the time and temperature of metal cation exchange reactions, to access a family of Cu(I)-MFU-4*l* (**I**–**VI**) with different Cu(I):Zn(II) ratios. **I**–**VI** were characterized using elemental analysis (EA), inductively coupled plasma-optical emission spectrometry (ICP-OES), powder X-ray diffraction (PXRD), and thermogravimetric analysis (TGA). Comparison of PXRD patterns (Figures S5–S10) reveal that all variants are isostructural and retain their crystallinity after cation exchange, with the exception of **VI**, which is prepared under elevated exchange temperature (100 °C) (Figure S11). EA and ICP-OES reveal Cu:Zn ratios of 1.2:3.8 (**I**), 1.8:3.2 (**II**), 2.2:2.8 (**III**), 2.3:2.7 (**IV**), 3:2 (**V**), and 3.8:1.2 (**VI**). Molecular formulas for **I**–**VI** were determined by combining the Cu and Zn analyses with CHN analyses (Supporting Information). TGA indicates that **I**–**V** decompose at the same temperature (~380 °C), which is comparable to MFU-4*l* (~410 °C) (Figures S12–S17).

N_2 adsorption isotherms (77 K) for **I**–**V** indicate permanent microporosity (Figures S18–S24). We observe, generally, that the Brunauer–Emmett–Teller (BET) surface areas decrease as a function of increased Cu(I) loading, achieved using either more prolonged cation exchange reaction times or increased cation exchange reaction temperatures (Table S5). The BET surface area and crystallinity of **VI**, in which nearly 80% of the Zn(II) have been replaced, decrease significantly; we therefore excluded **VI** from further studies. A detailed comparison of the experimental and simulated N_2 uptakes is provided in the Supporting Information. We postulate that lower than expected porosity for both pure MFU-4*l* and Cu(I) variants can be attributed to varying amounts of blocked pores or partial structural collapse.[29,30]

To investigate the effect of Cu(I) loading on olefin adsorption, ethylene adsorption isotherms were collected at 296 K (Figure S27). The net ethylene uptake increases with increased Cu(I) loading. For **I**–**V**, we observe a steep increase in ethylene uptake at very low pressures, followed by an abrupt change in slope and gradual increase to 1 bar (Figure S27). We attribute the initial steep uptake to ethylene binding to the open Cu(I) active sites and subsequent uptake to physisorption. The ethylene adsorption isotherm for pristine MFU-4*l* does not exhibit this steep increase at low pressures, indicating pure physisorption. For comparison, ethane adsorption isotherms for **I**–**V** were collected at 296 K (Figure S28). In each case, the ethane uptake at 1 bar was lower than that observed for pristine MFU-4*l*; the absence of a steep rise at low pressures is due to the lack of interaction with the Cu(I) sites. Decreasing ethane uptake from **I**–**V** is consistent with the observed decrease in BET surface area.

DOI: 10.1021/jacs.9b06582
J. Am. Chem. Soc. 2019, 141, 13003–13007

According to our calculations, the saturation limit for olefin chemisorption is one adsorbate per Cu(I). Assuming a defect-free system where every Cu is placed at a peripheral site, we calculated an upper limit for ethylene chemisorption (Figure S38). Here, the amount of chemisorbed ethylene is approximated by the uptake at 10 mmHg at 296 K (Figure S36). However, the observed total ethylene uptake is lower than the predicted capacity, indicating that ~55% of Cu atoms act as binding sites. Interestingly, the fraction of Cu atoms participating in chemisorption is independent of the Cu:Zn ratio. Additionally, Cu utilization does not appear to strongly correlate with changes in surface area (Figure S39). These observations motivated us to further investigate the nature of the Cu sites using continuous wave electron resonance (CW-EPR) spectroscopy. EPR detects only Cu(II) and is sensitive to the Cu(II) coordination environment. These studies are described in the Supporting Information. The data indicate the presence of saturated Cu(II) in the activated materials. Such sites would not coordinate olefin (Supporting Information) and explains at least part of the difference between calculated and experimental olefin uptake. X-ray photoelectron spectroscopy (Supporting Information) revealed a 0.9:0.1 Cu(I):Cu(II) ratio in activated **V**.

We next examined the single-site nature of the Cu(I) within **I**–**V** by measuring olefin-Cu(I) binding energies using temperature-programmed desorption (TPD) (Figures S49–S60). These measurements revealed that the ethylene desorption energies for **I**–**V** are very similar (Figure 2a).

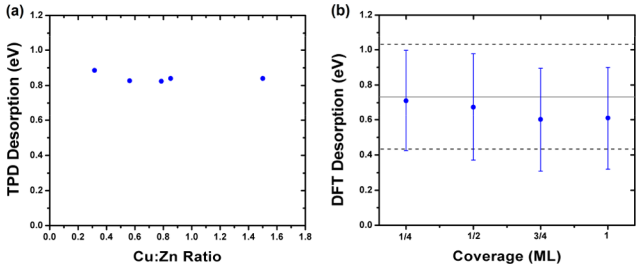

Figure 2. Ethylene desorption on Cu-MFU-4*l*. (a) TPD ethylene desorption energy on **I**–**V** as a function MOF Cu(I):Zn(II) ratio. (b) Calculated ethylene desorption (negative value of adsorption) energy on Cu-MFU-4*l*. The gray line represents the ethylene desorption energy at an SBU having Cu(I):Zn(II) ratio of 1:4 (1 peripheral Cu(I)). The blue points are for Cu(I):Zn(II) ratio of 4:1 (4 peripheral Cu(I)) at different ethylene coverage up to one monolayer (4 ethylene per SBU). The dashed lines and error bars represent $\pm\sigma$ from the BEEF-ensemble.

Desorption energies of 79.9 and 69 kJ/mol (for **V**) were observed for ethylene and propylene, respectively, which are within the range of binding energies observed for π-complexation adsorbents (60–120 kJ/mol), such as silver zeolite A[31] (95 kJ/mol) and PAF-1-SO_3Ag[14] (106 kJ/mol). These results match well with our ethylene desorption energies calculated at the extremes of Cu(I) loading (1 or 4 Cu(I) per SBU) (Figure 2b), indicating that the reactivity of each Cu(I) site is independent of the number of sites and that there are no interactions between neighboring sites. In addition, ethylene desorption was calculated at different coverages (blue points in Figure 2b), and coverage minimally impacts the binding energy (~0.1 eV) below 1 ML. Our calculations also show that a second ethylene molecule does not bind to an occupied Cu(I) site. This predicted lack of coverage effects is validated by the narrow range of binding energies observed in TPD, in sharp contrast to a typically broad range of binding energies on Cu surfaces due to adsorbate–adsorbate repulsion.[32] No adsorption was detected for ethane or propane. The high binding energies of ethylene and propylene enhance the olefin/paraffin separation factor, indicating the potential of these materials for the industrial separation of olefin/paraffin mixtures to obtain polymer-grade (>99.999%) olefins.

The separation capacity is confirmed in column breakthrough experiments performed on **V**, using equimolar ethylene/ethane and propylene/propane gas mixtures at ambient temperature and pressure (Figure 3). The mixed-gas

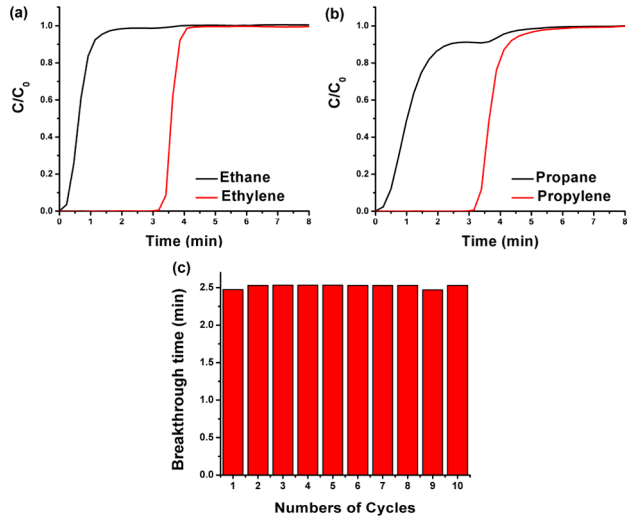

Figure 3. Olefin/paraffin separation performance of **V**. (a) and (b) Column breakthrough experiments for a diluted equimolar olefin/paraffin mixture (3:3:94 olefin/paraffin/nitrogen) on a packed column with ~50 mg **V** at a total flow rate of 10 sccm at 296 K and 1 bar. (c) Recycling experiments (10 cycles) using diluted equimolar ethylene/ethane mixture (5:5:90 ethylene/ethane/He).

samples were diluted using inert gas to enhance the time resolution of the experiment (3:3:94 olefin:paraffin:nitrogen); the mixture was introduced to a bed packed with ~50 mg of **V** (Supporting Information). Notably, paraffins were not adsorbed and were detected by mass spectrometry after a few seconds. In contrast, the olefins were retained in the bed for ~190 s (Figure 3a,b), confirming the capability of this material for efficient olefin/paraffin separation. The olefin can be regenerated from the fixed-bed via temperature–concentration swing recycling (TCSR) using an inert gas purge (helium, 20 sccm) at 140 °C for 20 min. Ethylene can be readily recovered from **V** with >99.999% purity without any observation of ethane during the regeneration process. Up to 10 cycles of ethylene/ethane adsorption/desorption measurements were performed using the breakthrough system and TCSR (Figures 3c, S61). **V** maintained its ethylene adsorption and regeneration capacity of 0.73 mol/kg over all regeneration cycles with complete molecular exclusion of ethane.

In summary, we demonstrated that introduction of unsaturated Cu(I) active sites into MFU-4*l* leads to materials that can efficiently separate olefin/paraffin mixtures to yield high-purity olefin. There remains opportunity to further optimize the synthesis of Cu(I)-MFU-4*l* to achieve significantly higher performance, as our theoretical predictions indicate that it is energetically feasible to completely substitute

DOI: 10.1021/jacs.9b06582
J. Am. Chem. Soc. 2019, 141, 13003–13007

Cu(I) atoms into all the peripheral Zn(II)-Cl sites. Because the sites are independent, performance for olefin/paraffin separations should increase linearly with further substitution.

■ ASSOCIATED CONTENT

Supporting Information

The Supporting Information is available free of charge on the ACS Publications website at DOI: 10.1021/jacs.9b06582.

Computational details, synthetic procedures, and material characterization (PDF)

■ AUTHOR INFORMATION

Corresponding Authors

*nrosi@pitt.edu
*karlj@pitt.edu
*gveser@pitt.edu

ORCID

Sunil Saxena: 0000-0001-9098-6114
J. Karl Johnson: 0000-0002-3608-8003
Nathaniel L. Rosi: 0000-0001-8025-8906

Notes

The authors declare no competing financial interest.

■ ACKNOWLEDGMENTS

This work was supported by the U.S. Department of Energy, Office of Science, Office of Basic Energy Science as part of the Computational Chemical Sciences Program, Award Number #DE-SC0018331. Computational support was provided by the University of Pittsburgh's Center for Research Computing and the Extreme Science and Engineering Discovery Environment (XSEDE), supported by National Science Foundation grant number ACI-1548562. Support for EPR instrumentation was provided by NSF MRI 1725678. Powder XRD measurements were collected at the Peterson Nanoscale Fabrication and Characterization Facility.

■ REFERENCES

(1) Czaja, A. U.; Trukhan, N.; Müller, U. Industrial applications of metal−organic frameworks. *Chem. Soc. Rev.* **2009**, *38*, 1284.
(2) Valvekens, P.; Vermoortele, F.; De Vos, D. Metal−organic frameworks as catalysts: the role of metal active sites. *Catal. Sci. Technol.* **2013**, *3*, 1435.
(3) Chen, B.; Yang, Y.; Zapata, F.; Lin, G.; Qian, G.; Lobkovsky, E. B. Luminescent Open Metal Sites within a Metal−Organic Framework for Sensing Small Molecules. *Adv. Mater.* **2007**, *19*, 1693.
(4) Chen, B.; Ockwig, N. W.; Millward, A. R.; Contreras, D. S.; Yaghi, O. M. High H_2 Adsorption in a Microporous Metal−Organic Framework with Open Metal Sites. *Angew. Chem., Int. Ed.* **2005**, *44*, 4745.
(5) Britt, D.; Furukawa, H.; Wang, B.; Glover, T. G.; Yaghi, O. M. Highly efficient separation of carbon dioxide by a metal-organic framework replete with open metal sites. *Proc. Natl. Acad. Sci. U. S. A.* **2009**, *106*, 20637.
(6) Lamia, N.; Jorge, M.; Granato, M. A.; Almeida Paz, F. A.; Chevreau, H.; Rodrigues, A. E. Adsorption of propane, propylene and isobutane on a metal−organic framework: Molecular simulation and experiment. *Chem. Eng. Sci.* **2009**, *64*, 3246.
(7) Eldridge, R. B. Olefin/paraffin separation technology: a review. *Ind. Eng. Chem. Res.* **1993**, *32*, 2208.
(8) Materials for Separation Technologies: Energy and Emission Reduction Opportunities 2005. https://www.osti.gov/servlets/purl/1218755.
(9) Cadiau, A.; Adil, K.; Bhatt, P. M.; Belmabkhout, Y.; Eddaoudi, M. A metal-organic framework−based splitter for separating propylene from propane. *Science* **2016**, *353*, 137.
(10) US Petrochemicals: The growing importance of export markets 2018. https://www.eia.gov/conference/2018/pdf/presentations/blake_eskew.pdf.
(11) Furukawa, H.; Cordova, K. E.; O'Keeffe, M.; Yaghi, O. M. The Chemistry and Applications of Metal-Organic Frameworks. *Science* **2013**, *341*, 1230444.
(12) Li, J.-R.; Kuppler, R. J.; Zhou, H.-C. Selective gas adsorption and separation in metal−organic frameworks. *Chem. Soc. Rev.* **2009**, *38*, 1477.
(13) Bloch, E. D.; Queen, W. L.; Krishna, R.; Zadrozny, J. M.; Brown, C. M.; Long, J. R. Hydrocarbon Separations in a Metal-Organic Framework with Open Iron(II) Coordination Sites. *Science* **2012**, *335*, 1606.
(14) Li, B.; Zhang, Y.; Krishna, R.; Yao, K.; Han, Y.; Wu, Z.; Ma, D.; Shi, Z.; Pham, T.; Space, B.; Liu, J.; Thallapally, P. K.; Liu, J.; Chrzanowski, M.; Ma, S. Introduction of π-Complexation into Porous Aromatic Framework for Highly Selective Adsorption of Ethylene over Ethane. *J. Am. Chem. Soc.* **2014**, *136*, 8654.
(15) Cui, X.; Chen, K.; Xing, H.; Yang, Q.; Krishna, R.; Bao, Z.; Wu, H.; Zhou, W.; Dong, X.; Han, Y.; Li, B.; Ren, Q.; Zaworotko, M. J.; Chen, B. Pore chemistry and size control in hybrid porous materials for acetylene capture from ethylene. *Science* **2016**, *353*, 141.
(16) Bachman, J. E.; Kapelewski, M. T.; Reed, D. A.; Gonzalez, M. I.; Long, J. R. M_2(m-dobdc) (M = Mn, Fe, Co, Ni) Metal−Organic Frameworks as Highly Selective, High-Capacity Adsorbents for Olefin/Paraffin Separations. *J. Am. Chem. Soc.* **2017**, *139*, 15363.
(17) Zhao, X.; Wang, Y.; Li, D.-S.; Bu, X.; Feng, P. Metal−Organic Frameworks for Separation. *Adv. Mater.* **2018**, *30* (37), 1705189.
(18) Bao, Z.; Wang, J.; Zhang, Z.; Xing, H.; Yang, Q.; Yang, Y.; Wu, H.; Krishna, R.; Zhou, W.; Chen, B.; Ren, Q. Molecular Sieving of Ethane from Ethylene through the Molecular Cross-Section Size Differentiation in Gallate-based Metal−Organic Frameworks. *Angew. Chem., Int. Ed.* **2018**, *57*, 16020.
(19) Lin, R.-B.; Li, L.; Zhou, H.-L.; Wu, H.; He, C.; Li, S.; Krishna, R.; Li, J.; Zhou, W.; Chen, B. Molecular sieving of ethylene from ethane using a rigid metal−organic framework. *Nat. Mater.* **2018**, *17*, 1128.
(20) Rogge, S. M. J.; Bavykina, A.; Hajek, J.; Garcia, H.; Olivos-Suarez, A. I.; Sepúlveda-Escribano, A.; Vimont, A.; Clet, G.; Bazin, P.; Kapteijn, F.; Daturi, M.; Ramos-Fernandez, E. V.; Llabrés i Xamena, F. X.; Van Speybroeck, V.; Gascon, J. Metal−organic and covalent organic frameworks as single-site catalysts. *Chem. Soc. Rev.* **2017**, *46*, 3134.
(21) Ranocchiari, M.; Lothschütz, C.; Grolimund, D.; van Bokhoven, J. A. Single-atom active sites on metal-organic frameworks. *Proc. R. Soc. London, Ser. A* **2012**, *468*, 1985.
(22) Denysenko, D.; Grzywa, M.; Tonigold, M.; Streppel, B.; Krkljus, I.; Hirscher, M.; Mugnaioli, E.; Kolb, U.; Hanss, J.; Volkmer, D. Elucidating Gating Effects for Hydrogen Sorption in MFU-4-Type Triazolate-Based Metal−Organic Frameworks Featuring Different Pore Sizes. *Chem. - Eur. J.* **2011**, *17*, 1837.
(23) Denysenko, D.; Jelic, J.; Reuter, K.; Volkmer, D. Postsynthetic Metal and Ligand Exchange in MFU-4l: A Screening Approach toward Functional Metal−Organic Frameworks Comprising Single-Site Active Centers. *Chem. - Eur. J.* **2015**, *21*, 8188.
(24) Dubey, R. J. C.; Comito, R. J.; Wu, Z.; Zhang, G.; Rieth, A. J.; Hendon, C. H.; Miller, J. T.; Dincă, M. Highly Stereoselective Heterogeneous Diene Polymerization by Co-MFU-4l: A Single-Site Catalyst Prepared by Cation Exchange. *J. Am. Chem. Soc.* **2017**, *139*, 12664.
(25) Comito, R. J.; Wu, Z.; Zhang, G.; Lawrence, J. A., III; Korzyński, M. D.; Kehl, J. A.; Miller, J. T.; Dincă, M. Stabilized Vanadium Catalyst for Olefin Polymerization by Site Isolation in a Metal−Organic Framework. *Angew. Chem., Int. Ed.* **2018**, *57*, 8135.

DOI: 10.1021/jacs.9b06582
J. Am. Chem. Soc. 2019, 141, 13003−13007

(26) Comito, R. J.; Metzger, E. D.; Wu, Z.; Zhang, G.; Hendon, C. H.; Miller, J. T.; Dincă, M. Selective Dimerization of Propylene with Ni-MFU-4l. *Organometallics* **2017**, *36*, 1681.
(27) Wellendorff, J.; Lundgaard, K. T.; Møgelhøj, A.; Petzold, V.; Landis, D. D.; Nørskov, J. K.; Bligaard, T.; Jacobsen, K. W. Density functionals for surface science: Exchange-correlation model development with Bayesian error estimation. *Phys. Rev. B: Condens. Matter Mater. Phys.* **2012**, *85*, 235149.
(28) Denysenko, D.; Grzywa, M.; Jelic, J.; Reuter, K.; Volkmer, D. Scorpionate-Type Coordination in MFU-4l Metal−Organic Frameworks: Small-Molecule Binding and Activation upon the Thermally Activated Formation of Open Metal Sites. *Angew. Chem., Int. Ed.* **2014**, *53*, 5832.
(29) Queen, W. L.; Hudson, M. R.; Bloch, E. D.; Mason, J. A.; Gonzalez, M. I.; Lee, J. S.; Gygi, D.; Howe, J. D.; Lee, K.; Darwish, T. A.; James, M.; Peterson, V. K.; Teat, S. J.; Smit, B.; Neaton, J. B.; Long, J. R.; Brown, C. M. Comprehensive study of carbon dioxide adsorption in the metal−organic frameworks M2(dobdc) (M = Mg, Mn, Fe, Co, Ni, Cu, Zn). *Chem. Sci.* **2014**, *5*, 4569.
(30) Haldoupis, E.; Borycz, J.; Shi, H.; Vogiatzis, K. D.; Bai, P.; Queen, W. L.; Gagliardi, L.; Siepmann, J. I. Ab Initio Derived Force Fields for Predicting CO_2 Adsorption and Accessibility of Metal Sites in the Metal−Organic Frameworks M-MOF-74 (M = Mn, Co, Ni, Cu). *J. Phys. Chem. C* **2015**, *119*, 16058.
(31) Aguado, S.; Bergeret, G.; Daniel, C.; Farrusseng, D. Absolute Molecular Sieve Separation of Ethylene/Ethane Mixtures with Silver Zeolite A. *J. Am. Chem. Soc.* **2012**, *134*, 14635.
(32) Grabow, L. C.; Hvolbæk, B.; Nørskov, J. K. Understanding Trends in Catalytic Activity: The Effect of Adsorbate−Adsorbate Interactions for CO Oxidation Over Transition Metals. *Top. Catal.* **2010**, *53*, 298.

DOI: 10.1021/jacs.9b06582
J. Am. Chem. Soc. 2019, 141, 13003−13007